

Resting-state networks in the infant brain

Peter Fransson^{†‡}, Beatrice Skiöld[§], Sandra Horsch^{§¶}, Anders Nordell[†], Mats Blennow^{||}, Hugo Lagercrantz[§], and Ulrika Åden[§]

[†]Magnetic Resonance Research Center, Department of Clinical Neuroscience, Stockholm Brain Institute, Karolinska Institute, SE-171 77 Stockholm, Sweden; [§]Neonatal Research Unit, Astrid Lindgren Children's Hospital, Karolinska Institute, SE-171 76 Stockholm, Sweden; [¶]Department of Neonatology, Erasmus MC-Sophia Children's Hospital, 3000 CB, Rotterdam, The Netherlands; and ^{||}Department of Clinical Science, Intervention, and Technology, Karolinska Institute, S-141 57 Huddinge, Sweden

Edited by Jean-Pierre Changeux, Institut Pasteur, Paris, France, and approved August 15, 2007 (received for review May 11, 2007)

In the absence of any overt task performance, it has been shown that spontaneous, intrinsic brain activity is expressed as system-wide, resting-state networks in the adult brain. However, the route to adult patterns of resting-state activity through neuronal development in the human brain is currently unknown. Therefore, we used functional MRI to map patterns of resting-state activity in infants during sleep. We found five unique resting-states networks in the infant brain that encompassed the primary visual cortex, bilateral sensorimotor areas, bilateral auditory cortex, a network including the precuneus area, lateral parietal cortex, and the cerebellum as well as an anterior network that incorporated the medial and dorsolateral prefrontal cortex. These results suggest that resting-state networks driven by spontaneous signal fluctuations are present already in the infant brain. The potential link between the emergence of behavior and patterns of resting-state activity in the infant brain is discussed.

development | functional MRI | spontaneous activity

Recent research on functional connectivity in the brain, in particular during resting-state conditions, has come to focus on low-frequency (<0.1 Hz), spontaneous fluctuations in the functional MRI (fMRI) signal. Discovered by Biswal *et al.* (1), it has been shown that systemwide networks in the resting brain are synchronized in time through intrinsic low-frequency signal fluctuations. Whereas early fMRI studies demonstrated synchronicity of intrinsic brain activity across hemispheres in primary sensory cortices (2, 3), succeeding studies have shown temporal synchronization in a resting-state network encompassing higher-order cortices (4). A systematic investigation of resting-state activity in the adult human brain was recently presented by Damoiseaux *et al.* (5). Using independent-component analysis (ICA), a data-driven explorative data analysis approach, they showed that there are numerous networks in the brain that are driven by spontaneous activity. Besides networks that are in part or fully described by the previously reported default mode (6) and task-positive network (7, 8), they found consistent patterns of resting-state activity in the visual cortex, sensorimotor areas, auditory areas, as well as extrastriate brain regions. These findings together with previous investigations on spontaneous activity suggest that the assumption that the brain during rest is idle and waiting to be triggered and respond to changes in the environment is not strictly valid. Rather, in addition to responding to changes in external stimuli or tasks, the brain is characterized by intrinsic dynamics in the form of coherent and spontaneous fluctuations, clustered together in networks that are credible from an anatomical and functional perspective.

Interestingly, recent studies have presented evidence that spontaneous activity is relevant for human behavior. Momentary lapses of attention, affecting goal-oriented behavior on a global/local selective attention task, were related to a failure to reduce activity in the default-mode network (9). Similarly, Fransson has shown that spontaneous, intrinsic activity in the default-mode network is markedly attenuated during a continuous verbal working memory task compared with rest (10). Moreover,

spontaneous activity was found to correlate with behavioral measures such as anxiety ratings and executive-control performance (11). In a similar vein, it has recently been reported that the amplitude of spontaneous activity in pain and attention-related brain regions correlates with the degree of experienced pain (12). In addition, potential relationships between spontaneous activity and disease have been investigated (13, 14).

So far, spontaneous activity has only been studied in adults with the exception of one study performed in children that was restricted in scope to the primary visual cortex (15). To our knowledge, spontaneous brain activity at an early developmental phase has not been addressed in the literature. To understand how cognitive circuits are developed in the human brain, we studied spontaneous brain activity by a systematic investigation of resting-state networks in the infant brain by using fMRI. Twelve preterm infants were scanned at term-equivalent age during sleep for 10 min. Physiologically relevant resting-state networks across subjects were extracted by using ICA. Additionally, the possibility that a negative finding might be the result of inadequate sensitivity was addressed by performing multiple resting-state scans on a healthy adult subject on the same MR scanner with identical scanning parameters.

Results

In individual subjects, anatomically coherent resting-state networks showed low-frequency BOLD fMRI signal changes <0.1 Hz, with the majority of the signal variance residing in the frequency range 0.01–0.05 Hz. In total, we could identify five resting-state networks in the infant brain. Representative spatial maps of resting-state networks in a single infant are shown in Fig. 1. Coherent patterns of spontaneous signal fluctuations at the individual level were typically observed in the medial section of the occipital lobe (Fig. 1A), bilaterally in the somatomotor cortex (Fig. 1B), bilaterally in the posterior temporal cortex (Fig. 1C), in the posterior medial and lateral parts of the parietal cortex (Fig. 1D), and in the anterior prefrontal cortex (Fig. 1E). The degree of temporal synchronicity of spontaneous BOLD signal changes across the hemispheres is shown in Fig. 2. Fig. 2A shows the temporal profile of BOLD signal oscillations in the bilateral somatomotor cortex during rest (see Fig. 1B), and the signal intensity time course in the bilateral posterior temporal cortex (see Fig. 1C) is shown in Fig. 2B.

Author contributions: P.F., M.B., H.L., and U.Å. designed research; P.F., B.S., S.H., and A.N. performed research; P.F. contributed new reagents/analytic tools; P.F. analyzed data; and P.F., H.L., and U.Å. wrote the paper.

The authors declare no conflict of interest.

This article is a PNAS Direct Submission.

Abbreviations: EPI, echo-planar imaging; fMRI, functional MRI; ICA, independent-component analysis; PICA, probabilistic independent-component analysis; WM, white matter.

[†]To whom correspondence should be addressed at: MR Research Center, N8, Department of Clinical Neuroscience, Karolinska University Hospital, SE-171 76 Stockholm, Sweden. E-mail: Peter.Fransson@ki.se.

This article contains supporting information online at www.pnas.org/cgi/content/full/0704380104/DC1.

© 2007 by The National Academy of Sciences of the USA

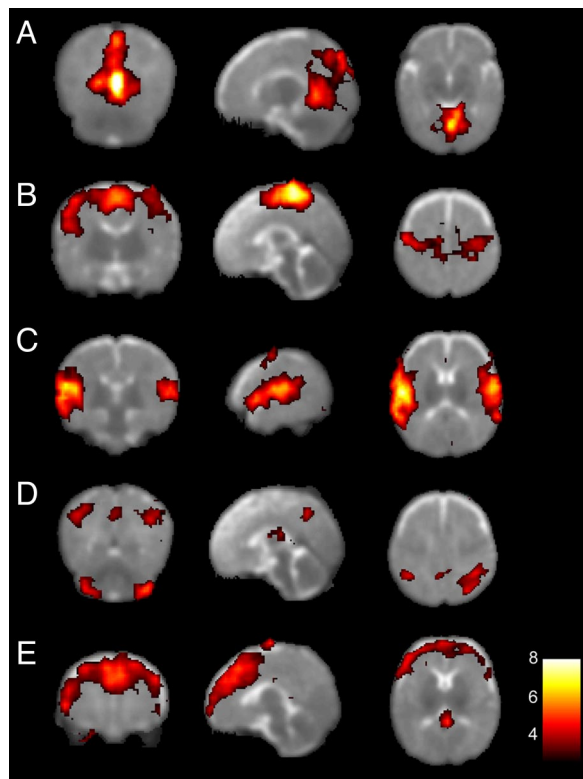


Fig. 3. Group resting-state networks in infants. Each row shows in a coronal, sagittal, and axial view resting-state networks thresholded at $P > 0.5$ (alternative-hypothesis threshold for activation vs. null) superimposed on a T2-weighted infant brain image template. Consistent resting-state patterns were found in the primary visual areas (A), somatosensory and motor cortices bilaterally (B), bilateral temporal/inferior parietal cortex encompassing the primary auditory cortex (C), posterior lateral and midline parts of the parietal cortex as well as the lateral aspects of the cerebellum (D), and medial and lateral sections of the anterior prefrontal cortex (E). The left side of the image corresponds to the left side of the brain.

connectivity that stretches out in the anterior–posterior direction. This discrepancy in the spatial configuration of resting-state patterns may be related to recent findings regarding white matter (WM) fiber tracts in infants. A diffusion tensor MR imaging investigation revealed a significantly lower anisotropy index in the inferior longitudinal fasciculus, inferior frontooccipital fasciculus, and superior longitudinal fasciculus compared with the detected degree of anisotropy in the interhemispheric callosal fibers (21), which suggests that the WM tracts that support functional connectivity in the anterior–posterior direction are less well developed in the infant brain compared with the tracts that support transcallosal functional connectivity (50).

The fact that resting-state patterns are largely confined to gray matter combined with the observation that the individual clusters are located in brain regions that collectively span system-wide, well known functional architectures in the brain suggests that coherent resting-state activity driven by low-frequency signal fluctuations is of functional relevance. It is interesting to compare our findings of intrinsic resting-state activity with results obtained from behavioral and conventional task-evoked neuroimaging studies in infants. Three of the five resting-state networks found in infants primarily involved brain areas that are known to be active for visual, auditory, and sensorimotor processing, respectively. To this end, task-evoked fMRI signal changes in response either to a reversing checkerboard (22) or to a flickering light (23) were observed in the primary visual cortex along the calcarine sulcus in sleeping infants. Moreover,

somatosensory areas in sedated infants were activated bilaterally in response to a unilateral, passive extension and flexion of the hand (24). In the case of auditory perception, activity in the temporal lobe has been reported for both simple tone stimuli in sleeping infants (25) as well as for speech processing in awake infants (26, 27). Our findings regarding resting-state activity together with previous results showing task-evoked responses are in agreement with positron-emission tomography investigations that have shown the highest degree of glucose metabolism in the primary sensory regions of the infant brain (28, 29).

There are two caveats to the present work. First, all data were collected in infants that were born preterm (gestational age <28 weeks). Although all infants were scanned at term-equivalent age and we took precautions to exclude subjects who showed signs of WM abnormalities or who otherwise showed abnormal brain development, it cannot be ruled out that preterm birth or perinatal factors as such might influence the observed patterns of resting-state activity in the infant brain. For example, diffusion tensor MRIs have detected subtle regional changes in specific WM regions, including the corpus callosum and internal capsule in unselected preterm infants at term compared with term-born infants (30, 31). Such abnormalities could potentially have influenced our results (see also refs. 32 and 33). On the other hand, the resting-state networks reported here clearly indicate that functional connectivity was present across the above-mentioned WM regions.

Second, resting-state networks were observed in slightly sedated and sleeping infants. To this end, a previous investigation that used transcranial magnetic stimulation and electroencephalography has shown that the cortical electrical activity after a magnetic pulse to the cortex does not spread along the cortical surface during sleep. This observation is in contrast to the sequence of spatial waves of activity in the cortex observed during quiet wakefulness (34). These results suggest that the loss of consciousness during sleep is caused by a breakdown of cortical connectivity during certain stages of sleep. On the other hand, a recent study has shown that the resting-state activity in the form of spontaneous, low-frequency BOLD fMRI signal changes persists and even is enhanced during the early stages of sleep (35). In a similar vein, the previous study by Kiviniemi *et al.* (15) showed that low-frequency, spontaneous fMRI signal changes in the primary visual cortex persist during sedation in children. In addition, speech sounds have been found to be learned by sleeping newborns as indicated by electrophysiological responses (36). We could detect resting-state patterns in primary sensory regions (Figs. 1A–C and 3A–C) that are in good agreement with data from awake adult subjects. Hence, it seems unlikely that sedation and/or sleep *per se* would account for the observed differences in resting-state patterns between infants and adults. Importantly, a recent study has presented convincing evidence that spontaneous brain activity in monkeys is preserved during anesthesia (37).

We failed to detect a direct equivalent of a default-mode network in the infant brain. There could be several reasons for this negative finding. It seems unlikely that it was caused by insufficient sensitivity in terms of signal to noise because all 10 previously described resting-state networks in adults could be detected in a single adult subject (see SI Fig. 4). As stated above, one cannot rule out the possibility that an absence of the default mode is related to subtle brain pathologies in the premature brain that were not visible on anatomical MR scans. However, we suggest that the absence of the default mode might be related to the relative immaturity of the infant brain. It has been suggested that the default-mode brain regions are primarily involved in self-referential processing, social cognition, and self-projection (38; for recent reviews, see refs. 39 and 40). Speculatively, the absence of a default-mode network might indicate that the neuronal processes responsible for self-

Table 1. Perinatal parameters for infants included in the work

Patient	Gender	BW, g	GA, weeks + days	GA at MRI	Delivery	BPD	PDA ligation	NEC	IVH grades 1 and 2	IVH grade 3, PHI, PHHC, PVL
1	M	755	26w2d	40w5d	CS	0	0	0	1	0
2	F	748	25w1d	40w1d	CS	1	1	0	1	0
3	M	882	25w4d	40w1d	VD	1	1	0	1	0
4	M	765	25w1d	40w4d	VD	0	0	0	0	0
5	F	948	25w6d	41w6d	VD	0	0	0	1	0
6	M	528	26w3d	41w4d	CS	0	0	0	0	0
7	M	1,325	27w5d	44w2d	VD	1	1	1	1	0
8	F	888	26w6d	42w0d	VD	0	0	0	0	0
9	F	499	25w1d	39w1d	CS	1	0	0	0	0
10	F	873	26w1d	40w0d	CS	0	0	0	0	0
11	M	660	24w4d	39w6d	CS	1	1	0	0	0
12	M	885	25w6d	41w5d	VD	1	1	0	0	0

Abbreviations: BW, birth weight; GA, gestational age; CS, cesarean section; VD, vaginal delivery; BPD, bronchopulmonary dysplasia (need for supplementary oxygen at 36 weeks postmenstrual age); PDA, patent ductus arteriosus; NEC, necrotizing enterocolitis; IVH, intraventricular hemorrhage; PHI, parenchymal hemorrhagic infarction; PHHC, posthemorrhagic hydrocephalus; PVL, periventricular leukomalacia.

processing and social interaction as well as mental projection in time have not matured in the infant brain. Although the network depicted in Fig. 3E shows similarities with the bilateral prefrontal resting-state network previously found in adults (5, 20), it also involves the medial prefrontal cortex. If one collapses the anterior (Fig. 3E) and the posterior (Fig. 3D) into one network and considers them collectively, they will together to some degree resemble the default-mode network. To test the hypothesis that the two networks are predecessors of the default-mode network, we performed a correlation analysis of the signal intensity time courses from the two networks in all subjects. The correlation analysis was computed from individual independent components selected on the basis of a spatial-correlation analysis (18). The correlation between the networks shown in Fig. 3D and E was not significant (Z score, -0.85 , $P > 0.1$), which would indicate that the anterior network in Fig. 3E is indeed related to the resting-state network described previously (5, 20). Rather, we speculatively suggest that the network encompassing the posterior parts of the default mode including the bilateral parietal cortex and the precuneus in Fig. 3D can tentatively be regarded as a proto-default-mode network in the infant brain. Moreover, Dehaene-Lambertz *et al.* (27) recently reported a distributed pattern of task-evoked signal deactivations in the medial occipital, superior frontal cortices and the caudate nuclei in 3-month-old infants in response to auditory presentation of sentences. The detected pattern of task-evoked deactivation was largely not in spatial agreement with the default-mode network commonly observed in adults.

The value of studying resting-state brain activity has recently been debated (41, 42). Although we do agree with Buckner and Vincent (42) in that activity driven by spontaneous fluctuations is a relevant area of research that adds to our knowledge of human brain function, contributes to our understanding of clinical conditions such as Alzheimer's disease, as well as potentially facilitates the study of comparative anatomy across species, we believe that in this work we have added a developmental aspect to the study of resting-state activity. Similar to the recent surge of interest in establishing links between spontaneous brain activity and behavior, we believe that the study of spontaneous activity in the brain at different time points along the early part of the human life span will contribute to our knowledge of how cognitive abilities are gradually developed and finally reach a mature form in the human brain.

In conclusion, by recording BOLD fMRI signals in sleeping infants we found that the infant brain hosts resting-state brain activity that showed both commonalities and disparities with

patterns previously reported for the adult brain. Whereas resting-state patterns in the visual, sensorimotor, and auditory regions in the infant brain showed large similarities with their adult counterparts, the default-mode network was not readily apparent in the infant brain.

Materials and Methods

Participants. The studied infants were part of an ongoing, population-based study of infants born at an extremely low gestational age. MRI was performed at a term-equivalent age. The MR images were analyzed by a neuroradiologist experienced in pediatric MRI. Only infants without overt WM lesions such as parenchymal hemorrhagic infarction (PHI) or periventricular leukomalacia (PVL) were eligible for this work. Low-grade intraventricular hemorrhages (IVH grades 1 and 2) were accepted. In addition, all scans were evaluated according to a scoring system for WM abnormalities regarding MRI signal abnormalities, reduction in WM volume, cysts, ventriculomegaly, myelination, and thinning of the corpus callosum (43). Only infants with normal WM according to the scoring system were included in the study (44). Thus, a total of 12 infants (5 girls and 7 boys) were recruited from the four neonatal units in Stockholm. The mean gestational age of the infants was 25 weeks and 6 days (range 24 weeks and 4 days to 27 weeks and 5 days) and mean birth weight was 813 g (range 499–1,325 g). Mean postmenstrual age at time of scanning was 41 weeks and 0 days (range 39 weeks and 1 day to 44 weeks and 2 days). Six of 12 infants were delivered by cesarean section. Three of 12 infants did not need any ventilatory support and were only treated with continuous positive airway pressure. Five of 12 infants had a low grade IVH, none had PHI, posthemorrhagic hydrocephalus, or PVL. Further perinatal details are given in Table 1.

The study was approved by the local ethical committee at the Karolinska University Hospital, and informed consent was obtained from all parents of the participating infants. A pediatrician stayed with the infant inside the scanner room throughout the imaging session to check on the infant's comfort. In agreement with our standard clinical protocol for neonatal MRI, infants were fed and given a low dose of the sedative agent chloral hydrate (30 mg/kg orally or rectally) with sustained spontaneous breathing, 15–30 min before MR scanning. Throughout the scanning session, arterial oxygen saturation and heart rate were continuously monitored.

MRI Acquisition. All MRI data were acquired on an Intera 1.5 T scanner with an 8-channel receive-only head coil (Philips, Best,

The Netherlands) at the Astrid Lindgren Children's Hospital in Stockholm. Anatomical high-resolution imaging included a T1-weighted turbo spin echo scan, an inversion recovery scan, as well as a three-dimensional gradient echo sequence (TR/TE/flip, 40 ms/4.6 ms/30 degrees; voxel size, $0.7 \times 0.7 \times 1 \text{ mm}^3$). Further, T2-weighted turbo spin echo images were acquired in both a sagittal and a coronal slice orientation. Functional MRI data were acquired by means of a gradient echo planar imaging (EPI) sequence sensitized to T2*-weighted signal changes (TR/TE/flip, 2,000 ms/50 ms/80 degrees). Whole-brain coverage was accomplished by acquiring 20 echo-planar images in an axial-slice orientation (FOV, 180 mm; matrix size, 64×64 ; thickness, 4.5 mm, interleaved slice acquisition order) yielding a spatial resolution of $2.8 \times 2.8 \times 4.5 \text{ mm}^3$. Resting-state functional connectivity was assessed by recording BOLD signal changes during 10 min of silent sleep (300 EPI image volumes). An additional four dummy scans were included to the beginning of the EPI acquisition to achieve steady-state magnetization. Because infants are more sensitive than adults to acoustic noise, particular care was taken to minimize exposure to high noise levels during MR scanning. In each infant, individually molded ear plugs (Affinis Dental Putty Soft; Forsberg Dental, Stockholm, Sweden) were used together with neonatal (MiniMuffs Natus Medical, Inc., San Carlos, CA) as well as pediatric ear muffs (Bilsom Junior; Bacou-Dalloz Nordic, Helsingborg, Sweden). To reduce the noise level inside the scanner even further, we used a tailor-made sound-dampening hood that was tightly attached to the upper half semicircle of the magnet bore, reducing the noise level with up to 24 dB (45). The total scanning time was $\approx 45\text{--}50$ min.

Image Preprocessing. As a first step, we used the BET algorithm included in the FSL (FMRIB, Oxford University, U.K.) software package to exclude all voxels that contained non-brain tissue from further analysis (46). Subsequent preprocessing steps were carried out within the SPM2 software package (Wellcome Trust Center for Neuroimaging, University College London, U.K.; ref. 47). Correction for subject movement was performed by realigning all EPI image volumes to the first image volume. Generally, subject movements were small both in terms of rotational and translational movement. However, in 6 of 12 subjects, the realignment procedure showed that the resting-state EPI datasets contained one, or in a few cases two, sudden and isolated "jerk-like" head movements, during which the infant's head was tilted away from its original position. Further, the realignment procedure showed that in all of these cases, within 10–20 s the infant tilted its head back into a position that was very close in space to its previous position. Because realignment correction algorithms are unable to cope with this sort of movement adequately, the affected image volumes were removed from the fMRI dataset, and the remaining image volumes were treated as one continuous dataset (mean no. of removed image volumes in affected datasets, 18; standard, 4 images). This procedure might be problematic in a stimulus-driven experimental design, but it has recently been shown that it is not detrimental in the context of analysis of low-frequency, spontaneous BOLD signal fluctuations (48). Subsequently, the realigned EPI data series were spatially normalized to an infant T2-weighted image template (26). Finally, all normalized EPI datasets were spatially smoothed by using a Gaussian isotropic filter with a full-width, half-maximum of 6 mm.

Image Analysis. At the individual level, spontaneous brain activity in the infant brain in the form of spatiotemporal resting-state patterns was extracted by using PICA (probabilistic independent-component analysis) as implemented in the MELODIC software within the FSL package (49). ICA is a data-driven, exploratory analysis tool that attempts to decompose the four-dimensional EPI datasets into separate components, based on the assumption that the spatial maps and their corresponding signal intensity time courses are statistically independent. Ideally, the resulting spatial maps will represent resting-state activation patterns and MR image artifacts of various kinds. Model-free approaches to data analysis such as ICA have previously been criticized because of the lack of interpretability and the possibility to do statistical inference testing. However, the PICA approach circumvents this problem by modeling the data as mixtures of spatially non-Gaussian signals and artifacts in the presence of Gaussian noise. Moreover, the overfitting problem, i.e., how many independent components that are present in the data, in PICA is handled by a dimensionality estimation procedure that is based on an objective assessment of the amount of Gaussian noise through Bayesian analysis of the data. Taken together, these methodological developments implemented in PICA allow a unique decomposition of the EPI data where each independent component is very likely to be the result of only one physical or physiological process (49).

The consistency of independent components across subjects was assessed by using a data concatenation approach that previously has been described by Beckmann *et al.* (20). In brief, the concatenation approach to multisubject analysis of resting-state patterns entailed as a first step a data reduction by forming a principal component analysis eigenbasis calculated from the mean data covariance matrix encompassing data from all 12 subjects. Second, the 30 most dominant eigenvectors obtained from the first step were used to project the individual dataset onto a dimensionality reduced data space. Third, an independent component analysis was performed on the temporally concatenated dataset, yielding 18 spatiotemporal patterns. The alternative hypothesis was tested at $P > 0.5$ for "activation" versus null, to create thresholded results for each resting-state network. A more detailed description of the concatenation approach to multisubject analysis of resting-state patterns is given in ref. 20.

We thank Johan Bengtsson and Dr. Lena Douglas for technical assistance and Dr. Christian Beckmann for statistical advice. H.L. was supported by a grant from the Torsten and Ragnar Söderberg Foundation. M.B. and S.H. were supported by grants from the Swedish Research Council (2006–6151), SLL (ALF 6076/os-226), the Jeansson Foundation, and the Swedish Medical Society. A.N. was supported by a grant from the Frimurare Foundations. P.F. was supported by a grant from the Karolinska Institute Research Foundation.

1. Biswal BB, Yetkin FZ, Haughton VM, Hyde JS (1995) *Magn Reson Med* 34:537–541.
2. Lowe MJ, Mock BJ, Sorenson JA (1998) *Neuroimage* 7:119–132.
3. Cordes D, Haughton VM, Arfanakis K, Carew JD, Turski PA, Moritz CH, Quigley MA, Meyerand ME (2001) *Am J Neuroradiol* 22:1326–1333.
4. Greicius MD, Krasnow B, Reiss AL, Menon V (2003) *Proc Natl Acad Sci USA* 100:253–258.
5. Damoiseaux JS, Rombouts SARB, Barkhof F, Scheltens P, Stam CJ, Smith SM, Beckmann CF (2006) *Proc Natl Acad Sci USA* 103:13848–13853.
6. Raichle ME, MacLeod AM, Snyder AZ, Powers WJ, Gusnard DA, Shulman GL (2001) *Proc Natl Acad Sci USA* 98:676–682.
7. Fransson P (2005) *Hum Brain Mapp* 26:15–29.
8. Fox MD, Snyder AZ, Vincent JL, Corbetta M, van Essen DC, Raichle ME (2005) *Proc Natl Acad Sci USA* 102:9673–9678.
9. Weissman DH, Roberts KC, Visscher KM, Woldorff MG (2006) *Nat Neurosci* 9:971–978.
10. Fransson P (2006) *Neuropsychologia* 44:2836–2845.
11. Seeley WW, Menon V, Schatzberg AF, Keller J, Glover GH, Kenna H, Reiss AL, Greicius MD (2007) *J Neurosci* 27:2349–2356.
12. Boly M, Balteau E, Schnakers C, Degueldre C, Moonen G, Luxen A, Phillips C, Peigneux P, Maquet P, Laureys S (2007) *Proc Natl Acad Sci USA* 104:12187–12192.
13. Greicius MD, Menon V (2004) *Proc Natl Acad Sci USA* 101:4637–4642.
14. Sonuga-Barke EJS, Castellanos FX (2007) *Neurosci Biobehav Rev* 31:977–986.

